

Synthesis and magnetic properties of Fe₃O₄ nanoparticles from the blast furnace flue dust

LAZHEN SHEN, YONGSHENG QIAO*, YONG GUO*, JIANGUO ZHAO

School of Chemistry and Chemical Engineering, Shanxi Datong University, Datong 037009, P. R. China

The Fe₃O₄ nanoparticles were prepared from a mixed solution of ferrous and ferric sulfate obtained by leaching the blast furnace (BF) flue dust with sulfuric acid. The factors affecting particle size, morphology, magnetic and other properties of Fe₃O₄ nanoparticles were investigated carefully. The phase structure, particle size and magnetic properties of the samples were characterized by means of X-ray diffraction (XRD) and transmission electron microscopy (TEM), vibrating sample magnetometer (VSM) and thermogravimetric differential thermal analyzer (TG-DTA). The results showed that the as-prepared Fe₃O₄ nanoparticles had pure phase, narrow size distribution, good dispersion and crystallinity, and exhibited the attractive magnetic property with high saturation magnetization of 105 emu/g. The synthesized magnetic materials show the potential application in the fields of information storage, biomedicine, catalyst, chemical sensors, etc.

(Received April 27, 2012; accepted July 11, 2013)

Keywords: Fe₃O₄, Nanoparticles, Magnetic properties, BF flue dust

1. Introduction

Magnetic nanomaterials have attracted much attention because of their fascinating properties and wide range of potential applications in biomedicine, information storage, catalyst, electromagnetic shielding, chemical sensors, and so on [1-5]. Among the nanomaterials, Fe₃O₄ nanoparticles have been widely studied for their excellent physical and chemical properties. However, these properties are greatly affected by the synthesis method, size and shape of Fe₃O₄ particles [6-8]. Various methods have been reported in the literature for the preparation of Fe₃O₄ nanoparticles [9-12], such as hydrothermal reaction of Fe²⁺ compounds, co-precipitation of Fe²⁺ and Fe³⁺ ions, microwave plasma synthesis method, and microemulsion method.

In this paper, a simple and effective method was developed to prepare Fe₃O₄ nanoparticles by recycling of the blast furnace (BF) flue dust produced from an iron and steel company, which not only makes full use of iron resource in the flue dust but also reduces environmental pollution. A mixed solution containing Fe²⁺ and Fe³⁺ ions was obtained by leaching the BF flue dust [13]. This mixed solution was used as the raw material for the synthesis of the Fe₃O₄ nanoparticles. Different experimental conditions, on which the size, shape and structures of Fe₃O₄ nanoparticles depended, were carefully studied. That provides a reference for the further preparation of the superparamagnetic Fe₃O₄ nanoparticles. The morphology, size distribution and other properties of the as-prepared Fe₃O₄ nanoparticles were characterized by XRD, TEM, VSM and TG-DTA. It was demonstrated that the obtained Fe₃O₄ nanoparticles have a narrow size distribution and good magnetic properties with high saturation magnetization (M_s).

2. Experimental

2.1 Synthesis of Fe₃O₄ nanoparticles

Fe₃O₄ nanoparticles were prepared by using the mixed solution of ferrous and ferric ions in an aqueous phase with NaOH as precipitant. Before preparation, the mole ratio of Fe³⁺/Fe²⁺ was adjusted in the range of 1.0:1-1.4:1. A 2.5 mol/L NaOH solution was added to the mixed solution until the solution pH up to 7.0-8.0 at room temperature. The whole mixture was stirred continuously to obtain a homogeneous solution. Then the solution was heated to above 80 °C. The color of solution changed from red brown to green gradually. The NaOH solution was added dropwise to the flask to keep pH of 7.0-8.0. When the above mixture turned black, the pH value was adjusted to 9.0-10.0 to make Fe²⁺ ions precipitate completely. Finally, the black precipitates collected were washed with distilled water and ethanol several times in an ultrasonic bath to remove any possible impurities. The black precipitates were dried at 70 °C for 10 h to obtain Fe₃O₄ nanoparticles.

2.2 Characterization

The powder X-ray diffraction (XRD) pattern was recorded using a BDX-3300 diffractometer equipped with Cu K α radiation ($\lambda = 1.5406 \text{ \AA}$) at room temperature. The measurement was performed at 40 kV and 20 mA from 20 to 70 ° with a 2θ scanning rate of 5 °/min and a step of 0.02 °. The morphology of the Fe₃O₄ nanoparticles was observed by transmission electron microscopy (TEM) using a BDX-3300 microscope (JEOL 100CX-II, Japan) at an accelerating voltage of 200 kV. TG-DTA curve was

characterized by a TA-50 (Japan) thermogravimetric differential thermal analyzer (TG-DTA) at a heating rate of 15 °C from room temperature to 975 °C under N₂ flow. Magnetic measurement was carried out on a USA LDJ 9600-1 vibrating sample magnetometer (VSM) at room temperature.

3. Results and discussion

3.1 TEM measurement

The TEM image of the obtained Fe₃O₄ nanoparticles is shown in Fig. 1. It is observed that the prepared nanoparticles are uniform spheres with good dispersion and a narrow particle size distribution. The average particle size of as-prepared Fe₃O₄ is about 50 nm.

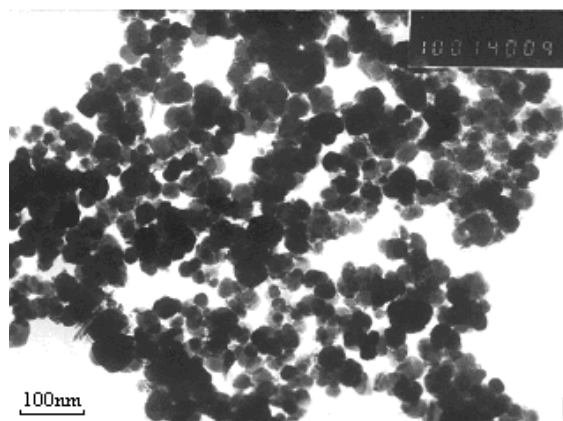


Fig. 1. TEM image of Fe₃O₄ nanoparticles.

3.2 XRD measurement

Fig. 2 shows a typical XRD pattern of as-prepared products. The XRD pattern indicates that the sample has five obvious diffraction peaks at 2θ of 30.1, 35.4, 42.9, 57.5 and 62.7, representing corresponding indices (220), (311), (400), (511) and (440), respectively of Fe₃O₄ [14]. The position and relative intensity of all diffraction peaks match well with the standard of Fe₃O₄ reflections, which reveals that the as-synthesized products exhibit an inverse spinel of pure Fe₃O₄ structure. No peaks of hematite, goethite, or other impurities are detected, suggesting the complete formation of Fe₃O₄ nanoparticles. The strong and sharp peaks reveal that Fe₃O₄ nanoparticles are well crystallized. The crystallite sizes are estimated from the five most intense peaks of the XRD pattern using Scherrer's equation. The calculated average value is 48.6 nm. The size of Fe₃O₄ particles calculated from the peak broadening in the XRD pattern is in good agreement with the size determined by TEM as shown in Fig. 1.

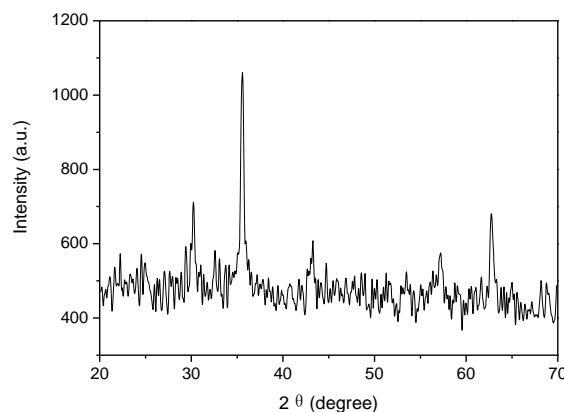


Fig. 2. XRD pattern of Fe₃O₄ nanoparticles.

3.3 Magnetic measurement

Fe₃O₄ has exhibited unique electric and magnetic properties based on the transfer of electrons between Fe²⁺ and Fe³⁺ ions in the octahedral sites. Magnetic measurement of the as-prepared Fe₃O₄ nanoparticles was conducted at room temperature, and the magnetic hysteresis (M–H) loop was presented in Fig. 3.

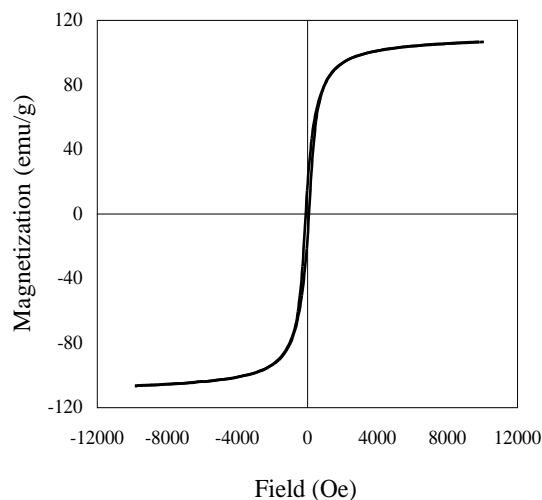


Fig. 3. Magnetic hysteresis loop of Fe₃O₄ nanoparticles.

The hysteresis loop of the product shows the ferromagnetic behavior with saturation magnetization of 105 emu/g and coercivity values (H_c) of 100 Oe, respectively. The M_s is larger than that of bulk Fe₃O₄ (90 emu/g) and the H_c is smaller than that of bulk Fe₃O₄ (115 Oe) [15]. The M_s and H_c values are affected by the size, shape, crystal structure and surface state of Fe₃O₄ particles [16]. The increase in M_s value in this paper may be due to the good crystallinity and lower surface-to-volume ratio. The reduced H_c value can be caused by the anisotropy, including crystal anisotropy and shape anisotropy, which plays an important role in reducing coercivity [17].

3.4 TG-DTA measurement

The dehydration process and oxidation process of Fe₃O₄ particles were analyzed by TG-DTA method. The TG-DTA curves are shown in Fig. 4. From Fig. 4a, it is clear that there are three endothermic peaks on DTA curve of dehydration process. The first endothermic peak at about 100 °C corresponds to the adsorbed water of the sample. The second endothermic peak at about 235 °C is assigned to the crystal water within Fe₃O₄ crystal. The third endothermic peak at about 345 °C is the structure water of the sample. The former two waters exist in the form of free molecules. Usually, the removal of adsorbed water is about 100 °C, and the crystal water is dehydrated at a higher temperature because crystal water is packed in the crystal lattice and is affected by the impact of grain boundary barriers. Therefore, the results of TG-DTG show the crystalline water is dehydrated at about 235 °C. Structure water is a component of Fe₃O₄ molecular with the form of hydroxyl (-OH) or H₃O⁺. It has fixed water content and determined coordination position, only the high temperature can break the chemical bonds to get off, meanwhile, structure water is dehydrated mostly in single molecular form so that no hole will be left in the crystal. The maximum weight loss at 100 °C indicates that the adsorbed water accounts for the most content of total water.

The TG curve as illustrated in Fig. 4b shows that Fe₃O₄ particles have two weight gain steps and one weight loss peak from 150 °C to 975 °C. TG curve shows that the oxidation rate is slow before 200 °C owing to the unobvious weight gain trend. Then the oxidation rate speeds up gradually, and a clear weight gain peak at 234 °C is due to the oxidation of Fe₃O₄ to γ -Fe₂O₃. The subsequent TG curve shows a slower rate of decline. There is a significant weight gain peak at 515 °C (Curie temperature of γ -Fe₂O₃ T_C = 575 °C [18]), that indicates the all Fe₃O₄ phase disappear and are converted to γ -Fe₂O₃. A weight loss at about 765 °C (Curie temperature of α -Fe₂O₃ T_C = 747 °C) resulting from the disappearance of spinel crystal is observed because of the change from γ -Fe₂O₃ phase to α -Fe₂O₃ phase. DTA curve shows that the oxidation process of Fe₃O₄ is an exothermic process. The obvious exothermic peak at 234 °C corresponds to the weight gain peak on TG curve, which indicates the formation of spinel phase. The slow endothermic period after this is the lattice correction period. The exothermic peak at 765 °C also shows the disappearance of γ -Fe₂O₃ phase while the formation of α -Fe₂O₃ phase. Then DTA curve shows the adsorption process after the exothermic peak at 765 °C owing to the rearrangement of α -Fe₂O₃ lattice.

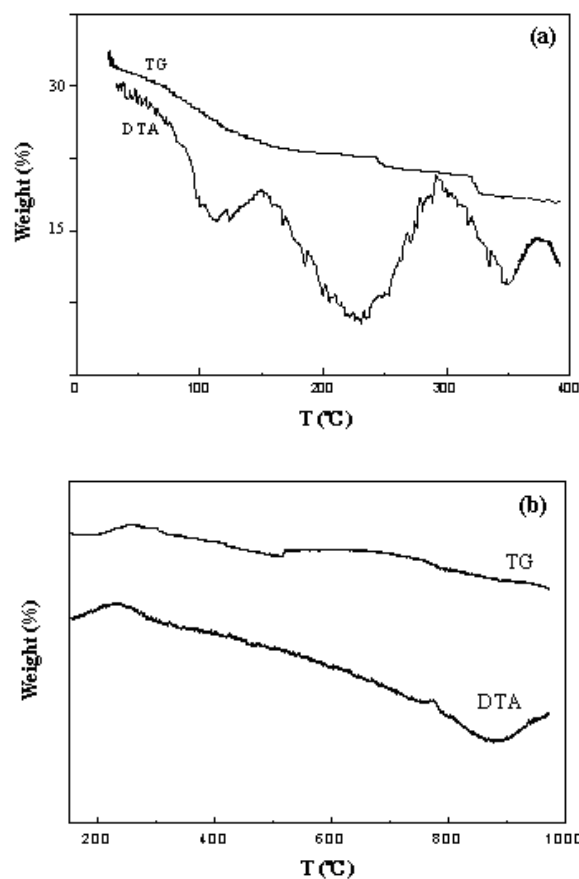


Fig. 4. TG-DTA curves during (a) dehydration process and (b) oxidation process of Fe₃O₄ nanoparticles.

The size, shape, structure and composition of resultant products are determined on many factors, such as reaction temperature, concentration of solution, pH value, reaction time, crystallization, volume of air, etc. Generally speaking, temperature, pH value, the adding way of precipitant and volume of air have great influence on the structure and composition of final products. The temperature of 80 °C -95 °C is in favor of the formation of Fe₃O₄ phase. Because the diffusion rate of Fe(II) is fast at high temperature, part of Fe(II) ions without time were oxidized to Fe(III) and then enter the lattice to produce Fe₃O₄ phase. When temperature is lower than 50 °C, the diffusion rate of Fe(II) is slow. Fe(II) ions have enough time to be oxidized to Fe(III), that brings some FeOOH phase to generate impure Fe₃O₄ phase. It is better for the formation of Fe₃O₄ particles at the higher pH value. At pH lower than 4.9, it is easy to form FeOOH rather than Fe₃O₄ [19]. Therefore, the precipitant should be added in iron salt solution in one time to make pH up to 7-8, this pH value is benefit for the formation of Fe₃O₄. The XRD patterns of the samples obtained at high pH and low pH respectively are shown in Fig. 5a and b. It can be seen that the product prepared at high pH matches well with the standard Fe₃O₄ reflections. However, Fig. 5b shows a weak diffraction peak intensity of Fe₃O₄, and part peaks can be assigned to

FeOOH and Fe₂O₃ phases. It indicates the pH value has great effect on the purity of product. The ventilation volume is another important factor that has influence on the composition of resultant products. As the oxidation reaction is carried out on the surface of the air bubbles. The increase of effective air flow will generate more bubbles and then increase the oxidation degree of Fe(II). More FeOOH phase will be obtained in the final products. When the effective air flow decreases even no air enters into the solution, the concentration of Fe(III) ions decreases and produces pure Fe₃O₄ phase.

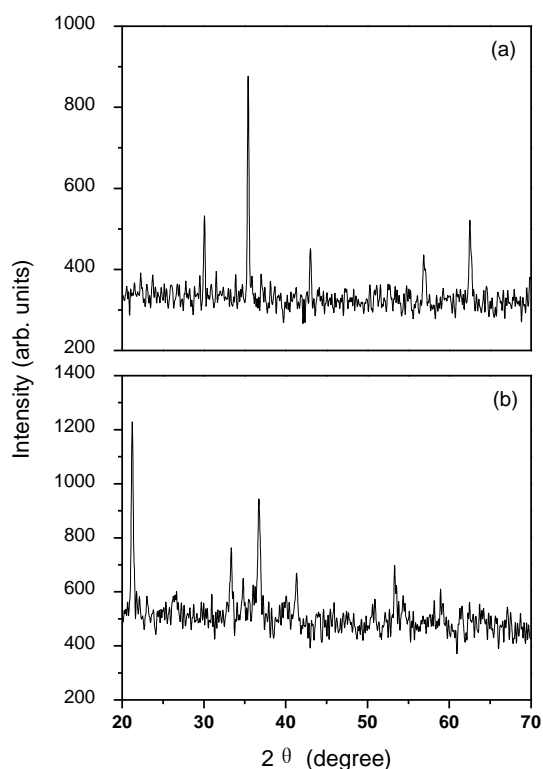


Fig. 5. XRD patterns of Fe₃O₄ nanoparticles prepared at (a) high pH and (b) low pH.

The size of Fe₃O₄ particles is affected by the concentrations of iron ions and precipitant as well as crystallization. Too high or too low concentration is unfavorable to the formation of a uniform particle size and high crystallization degree. Grains have enough time to grow up to form the good crystalline degree but large size of particles at low concentration. Contrary to low concentration, a large amount of grains will generate quickly in high concentration, which results in the very fine but imperfect crystalline degree particles. Under the moderate concentration, it is beneficial to the homogenous distribution of the air in solution and uniform nucleation of grain, and there is enough time to grow, these factors lead to a narrow size distribution with good crystalline degree and pronounced magnetite structure according to the strong diffraction peak in XRD pattern as shown in Fig. 2.

According to nucleation growth mechanism, the large ventilation volume will generate more nucleation centers and increase crystallization rate under the other conditions unchanged, which results in small size of grain, conversely, the larger grain size will be obtained. Crystallization temperature and time also have great influence on the particle size and size distribution. Crystallization process is the process of grain growth, during this process, the small grains gradually dissolve and larger grains grow slowly. Fig. 6 exhibits the change of particle size with the crystallization temperature. It can be observed that the particle size increases with the increase of crystallization temperature. The TEM image of Fe₃O₄ nanoparticles obtained by using a higher crystallization temperature than that of the sample as shown in Fig. 1 is given in Fig. 7. Due to the slow crystal growth, the crystal defects are made up and grain size become uniform. After the crystallization, the crystal particle surface becomes smooth, crystal integrity also has been improved, particle size is larger and the size distribution is more homogenous (Fig. 7) compared with Fig. 1. On the other hand, the increase in reaction temperature is also in favor of the growth of the particle size.

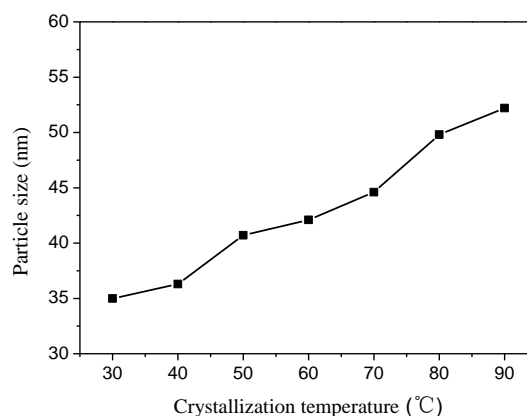


Fig. 6. Change of particle size with crystallization temperature.

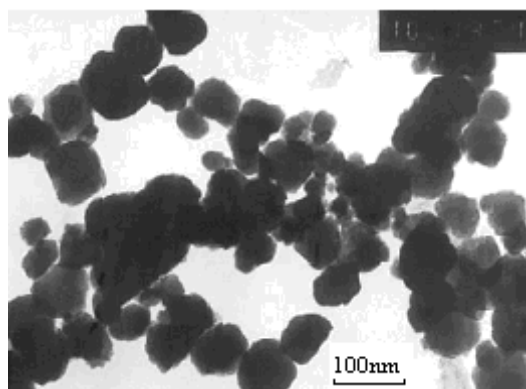


Fig. 7. TEM image of Fe₃O₄ nanoparticles obtained at higher crystallization temperature.

4. Conclusions

This paper put forward a simple method to prepare Fe₃O₄ nanoparticles by recycling of the blast furnace (BF) flue dust produced from an iron and steel company, which not only makes full use of iron resource in the flue dust but also reduces environmental pollution. A mixed solution of Fe²⁺ and Fe³⁺ ions was obtained by leaching BF flue dust. This mixed solution was used as raw material for the synthesis of Fe₃O₄ nanoparticles. The factors influencing the particle size, composition, morphology and magnetic properties of Fe₃O₄ nanoparticles were discussed in detail. The average size of obtained Fe₃O₄ particles was about 50 nm. The characterization results indicated that the as-prepared Fe₃O₄ nanoparticles exhibited a narrow size distribution, good dispersion, regular nanostructure, pure phase and high saturation magnetization. The synthesized magnetic Fe₃O₄ nanoparticles may have important potential applications in advanced magnetic materials, biomedical fields and other fields.

Acknowledgment

The authors are thankful to the supports of the Scientific and Technological Innovation Programs of Higher Education Institutions in Shanxi, China (no. 20121017), the National Natural Science Foundation of China (nos. 21073113 and 51072105), the Natural Science Foundation for Young Scientists of Shanxi Province, China (no. 2012021020-5), and Dr. Starting funds research of Shanxi Datong University (no. 2008-B-20).

References

- [1] Y. F. Zhu, T. Ikoma, N. Hanagata, S. Kaskel, *Small* **6**, 471 (2010).
- [2] F. H. Chen, L. M. Zhang, Q. T. Chen, Y. Zhang, Z. J. Zhang, *Chem. Commun.* **46**, 8633 (2010).
- [3] Y. Chen, H. Y. Chen, D. P. Zeng, Y. B. Tian, F. Chen, J. W. Feng, J. L. Shi, *ACS Nano* **4**, 6001 (2010).
- [4] H. Karami, *Chem. Eng. J.* **219**, 209 (2013).
- [5] A. S. Teja, P. Y. Koh, *Prog. Cryst. Growth. Ch.* **55**, 22 (2009).
- [6] M. Abbas, M. Takahashi, *J. Nanopart. Res.* **15**, 1354 (2013).
- [7] S. Laurent, D. Forge, M. Port, A. Roch, C. Robic, L. V. Elst, R. N. Muller, *Chem. Rev.* **108**, 2064 (2008).
- [8] J. Park, G. von Maltzahn, L. Zhang, M. P. Schwartz, E. Ruoslahti, S. N. Bhatia, M. J. Sailor, *Adv. Mater.* **20**, 1630 (2008).
- [9] T. Togashi, M. Umetsu, T. Naka, S. Ohara, Y. Hatakeyama, T. Adschiri, *J. Nanopart. Res.* **13**, 3991 (2011).
- [10] M. M. Rashad, H. M. El-Sayed, M. Rasly, M. I. Nasr, *J. Magn. Magn. Mater.* **324**, 4019 (2012).
- [11] G. H. Gao, R. R. Shi, W. Q. Qin, Y. G. Shi, G. F. Xu, G. Z. Qiu, X. H. Liu, *J. Mater. Sci.* **45**, 3483 (2010).
- [12] Z. Li, B. Tan, M. Allix, A. I. Cooper, M. J. Rosseinsky, *Small* **4**, 231 (2008).
- [13] L. Z. Shen, Y. S. Qiao, Y. Guo, J. R. Tan, *J. Hazard. Mater.* **177**, 495 (2010).
- [14] K. Aslam, *Mater. Lett.* **62**, 898 (2008).
- [15] J. Y. Jing, Y. Zhang, J. Y. Liang, Q. B. Zhang, E. Bryant, C. Avendano, V. L. Colvin, Y. D. Wang, W. Y. Li, W. W. Yu, *J. Nanopart. Res.* **14**, 827 (2012).
- [16] K. Y. Yoon, C. Kotsmar, D. R. Ingram, C. Huh, S. L. Bryant, T. E. Milner, K. P. Johnston, *Langmuir* **27**, 10962 (2011).
- [17] R. P. Patil, P. P. Hankare, K. M. Garadkar, R. Sasikala, *J. Alloy. Compd.* **523**, 66 (2012).
- [18] Z. Liu, *Ferromagnetic Material Magnetic Ordered Material Properties Handbook* (vol. II), Electronic Industry Press, Beijing (1993).
- [19] T. Misawa, K. Hashimoto, S. Shimodaira, *Corros. Sci.* **14**, 131 (1974).

*Corresponding author: dtdxqys@163.com, ybsy_guo@163.com